

# Oriented gap opening in the magnetically ordered state of Iron-pnictides: an impact of intrinsic unit cell doubling on the $Fe$ square lattice by $As$ atoms

Ningning Hao,<sup>1,2</sup> Yupeng Wang,<sup>1</sup> and Jiangping Hu<sup>1,2</sup>

<sup>1</sup>Beijing National Laboratory for Condensed Matter Physics and Institute of Physics, Chinese Academy of Sciences, P. O. Box 603, Beijing 100190, China

<sup>2</sup>Department of Physics, Purdue University, West Lafayette, Indiana 47907, USA

We show that the complicated band reconstruction near Fermi surfaces in the magnetically ordered state of iron-pnictides observed by angle-resolved photoemission spectroscopies (ARPES) can be understood in a meanfield level if the *intrinsic unit cell doubling* due to As atoms is properly considered as shown in the recently constructed  $S_4$  microscopic effective model. The  $(0,\pi)$  or  $(\pi,0)$  col-linear antiferromagnetic (C-AFM) order does not open gaps between two points at Fermi surfaces linked by the ordered wave vector but forces a band reconstruction involving four points in unfolded Brillouin zone (BZ) and gives rise to small pockets or hot spots. The  $S_4$  symmetry naturally chooses a staggered orbital order over a ferro-orbital order to coexist with the C-AFM order. These results strongly suggest that the kinematics based on the  $S_4$  symmetry captures the essential low energy physics of iron-based superconductors.

PACS numbers: xxx

*Introduction:* The parent compounds of all Iron-pnictide high temperature superconductor[1–3] are characterized by a unique C-AFM order[4–6]. In the past several years, although the majority of theoretical studies on these compounds have successfully obtained such a magnetic state from both itinerant and local moment models[7–14], the band reconstruction in the C-AFM state observed by ARPES[15–18] remains a puzzle. Unlike in a conventional spin density wave (SDW) state where gaps at any two points at Fermi surfaces which are connected by the ordered SDW wave vector should be opened generically, the band structure in the C-AFM state appears to be reconstructed by the development of the magnetic order. While optical measurements suggest a significant portion of Fermi surfaces are gapped[19–22], ARPES observes that small pockets or hot spots develop around Fermi surfaces. It is fair to say that the scenario of the gap opening due to a magnetic order in a multi-orbital system, such as iron-pnictides, is complex. For example, it has been argued that the entire Fermi surfaces can be gaped out[23]. Nevertheless, the surprising band reconstruction is never clearly understood until now.

In this paper, we demonstrate that in the recently constructed effective two-orbital model with the  $S_4$  symmetry, which is the symmetry of the trilayer FeAs structure, the band reconstruction becomes a natural consequence from the intrinsic unit cell doubling due to As atoms[24]. The spirit of the  $S_4$  model is that the kinematics can be divided into weakly coupled two orbital models controlled separately by two  $S_4$  iso-spin components as shown in Fig.1(a). For each  $S_4$  iso-spin component, a unit cell includes two irons, namely, the unit cell is doubled, and the doubling results in the formation of a pair of bands which are responsible for a hole pocket at  $\Gamma$  and an electron pocket at  $M$ . Although this kinematics is hidden in various multi-orbital models constructed for iron-based superconductors as shown in[24]. Here we show that it is the extraction of such a minimum effective model allows us to naturally capture the band reconstruction features mentioned above in a simple mean-field Hamiltonian. The  $S_4$  symmetry also naturally imposes a staggered orbital order over a ferro-orbital order to co-

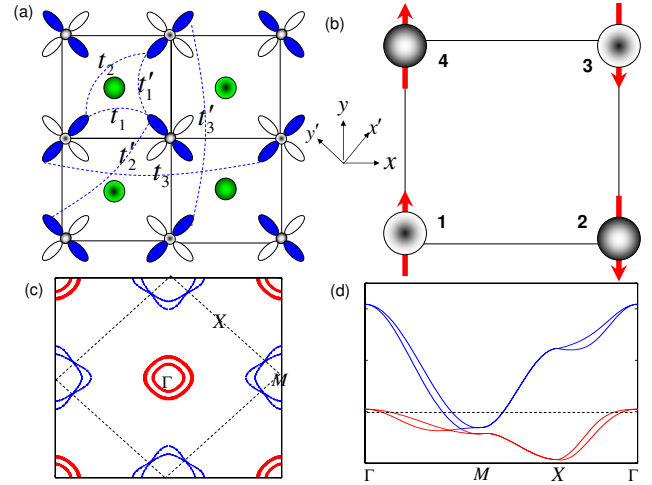


FIG. 1: (color online) (a) The lattice structure of Fe-As trilayers. The different filled green/big balls indicate the top and bottom As layer. The blue/deep and white/light orbital patterns indicate two  $S_4$  iso-spin components. The effective hopping parameters up to 3rd nearest neighbor are marked. (b) The  $(\pi, 0)$  C-AFM order are shown. Four Fe sublattices in the unit cell of C-AFM state are marked. (c) and (d) The Fermi surfaces and energy spectrums along high symmetric lines for normal paramagnetic state are shown. The hopping parameters are set  $t_1 = 0.47$ ,  $t'_1 = 0.53$ ,  $t_2 = 0.9$ ,  $t'_2 = -0.18$ ,  $t_3 = 0.0$ ,  $t'_3 = 0.1$ ,  $t_c = 0.1$  and  $\mu = -0.5$  for electron underdoped 4.5%.

exist with the C-AFM order. *Our results suggest that a proper starting point in kinematics is crucial to obtain a correct meanfield result and the kinematics based on  $S_4$  symmetry due to As atoms provides the essential low energy physics of iron-based superconductors.*

*Oriented gap opening mechanism with unit cell doubling:* The effect of the unit cell doubling on the C-AFM state can be elucidated by considering the kinematics of a single  $S_4$  iso-spin component. Deeply in a C-AFM state, regardless of the origin of the magnetic ordering, we should expect that a SDW order can capture the basic features of itinerant bands. As shown in Fig.1(a), the kinematics of the single blue (deep) orbital

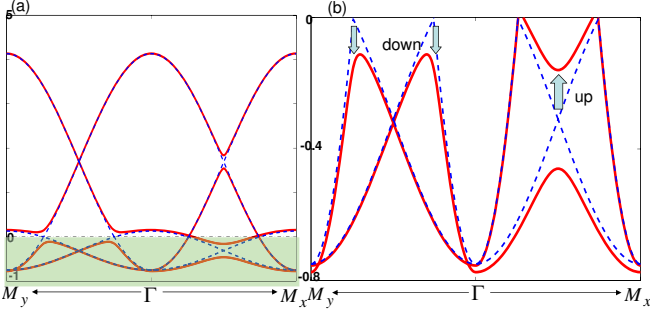


FIG. 2: (color online) (a) The energy bands of Hamiltonian Eq. (1) with spin-up component in  $(\pi, 0)$  C-AFM state along  $\Gamma - M_x$  and  $\Gamma - M_y$  directions are shown. The blue/dashed lines indicate the normal state while the red/solid lines indicate the C-AFM state. The shadow regime indicates the parts below Fermi surfaces. (b) The shadow regime in (a) is zoomed in. The arrows indicate the bands in C-AFM state shift up or down compared with that in normal state. We set  $t_1 = t'_1 = 0.5$ ,  $t_2 = 0.9$ ,  $t'_2 = -0.18$ ,  $t_3 = t'_3 = 0.0$ ,  $\mu = -0.69$  and  $\Delta_{SDW} = 0.15$ .

has an intrinsic unit cell doubling due to the large difference between the two next nearest neighbor hopping parameters,  $t_2$  and  $t'_2$  (note: the details of the  $S_4$  model can be found in our previous paper[24]).

In the  $Q_1 = (\pi, 0)$  C-AFM state shown in Fig. 1 (b), at the 1 and 4 sites, the spin-up component is a majority while at the sites 2 and 3, the spin-down component is a majority. A simple SDW order is thus given by  $\Delta_{SDW} = \langle \sum_{k\sigma} \eta_\sigma c_{k,\sigma}^\dagger c_{k+Q_1,\sigma} \rangle$  where  $\eta_\uparrow = 1$  and  $\eta_\downarrow = -1$  for different spin components. Due to the intrinsic unit cell doubling, for any given point  $k$  in unfolded BZ zone, there are four momenta linked in the presence of the magnetic order,  $k, k + Q_1, k + Q$ , and  $k + Q_2$  where  $Q = (\pi, \pi)$  and  $Q_2 = (0, \pi)$ . The mean-field Hamiltonian that described the  $(\pi, 0)$  C-AFM state can thus be expressed as  $H = \sum_{k,\sigma} \psi_{k,\sigma}^\dagger \mathcal{H}(k, \sigma) \psi_{k,\sigma}$  with  $\psi_{k,\sigma} = [c_{k,\sigma}, c_{k+Q,\sigma}, c_{k+Q_1,\sigma}, c_{k+Q_2,\sigma}]^T$ .  $\mathcal{H}(k, \sigma)$  is given by

$$\mathcal{H}(k, \sigma) = \begin{bmatrix} f(k) & g(k) & \eta_\sigma \Delta_{SDW} & 0 \\ g^*(k) & f(k+Q) & 0 & \eta_\sigma \Delta_{SDW} \\ \eta_\sigma \Delta_{SDW} & 0 & f(k+Q_1) & g(k+Q_1) \\ 0 & \eta_\sigma \Delta_{SDW} & g^*(k+Q_1) & f(k+Q_2) \end{bmatrix} \quad (1)$$

where  $f(k) = 2t_{1s}(\cos k_x + \cos k_y) + 2t_{1d}(\cos k_x - \cos k_y) + 4t_{2s} \cos k_x \cos k_y + 2t_{3s}(\cos 2k_x + \cos 2k_y) + 2t_{3d}(\cos 2k_x - \cos 2k_y) - \mu$ ,  $g(k) = 4t_{2d} \sin k_x \sin k_y$  and  $t_{is} = (t_i + t'_i)/2$ ,  $t_{id} = (t_i - t'_i)/2$  with  $i = 1, 2, 3$ . It is explicit to find that the spin-up and spin-down electrons play a symmetrical role in building up the  $(\pi, 0)$  C-AFM states. Hence, we can only investigate  $\mathcal{H}(k, \uparrow)$ .

Now we are in a position to show that the gap opening described in Eq.1 is rather different from a conventional one in a conventional SDW state. Here the energy dispersions of  $\mathcal{H}(k, \uparrow)$  can not be given by a simple analytical form. We provide the numerical results for spin-up case shown in Fig. 2. It is easy to see that the band reconstruction in the C-AFM state are anisotropic along the  $\Gamma - M_x$  and  $\Gamma - M_y$  directions. Below Fermi surfaces, an energy splitting takes place between two hole bands at

$(\frac{\pi}{2}, 0)$  point along the  $\Gamma - M_x$ . Along the  $\Gamma - M_y$  direction, gaps at Fermi surfaces are opened between a hole band and an electron band. Due to the fact that the gap openings are different along different directions, we call this behavior as *oriented gap opening*. As we will show later, this behavior leads to a development of hot spots or a small pockets on Fermi surfaces.

*The self-consistent mean-field results:* In the above analysis, the magnetic order is introduced artificially. To show the magnetic order is generated by standard interactions in the  $S_4$  model (note, a recent quantum monte carlo calculation has already shown the C-AFM correlation is the leading magnetic correlation of the model near half filling[11]) as well as to produce more realistic results that can be closely compared to ARPES observations, we apply a self-consistent meanfield calculation to consider the full  $S_4$  model with the full interaction terms.

Including all possible electron-electron interaction terms, the general Hamiltonian of the  $S_4$  model is given by[24],

$$H = H_0 + H_{int} \quad (2)$$

where  $H_0$  is the kinematics part given in[24] and

$$\begin{aligned} H_{int} = & U \sum_{i,\alpha} (\hat{n}_{i\alpha\uparrow}^c \hat{n}_{i\alpha\downarrow}^c + \hat{n}_{i\alpha\uparrow}^d \hat{n}_{i\alpha\downarrow}^d) + U' \sum_{i,\alpha,\sigma} \hat{n}_{i\alpha\sigma}^c \hat{n}_{i\alpha\sigma}^d \\ & + (U' - J_H) \sum_{i,\alpha,\sigma} \hat{n}_{i\alpha\sigma}^c \hat{n}_{i\alpha\sigma}^d \\ & + J_H \sum_{i,\alpha} (c_{i\alpha\uparrow}^\dagger d_{i\alpha\downarrow}^\dagger c_{i\alpha\downarrow} d_{i\alpha\uparrow} + c_{i\alpha\uparrow}^\dagger c_{i\alpha\downarrow}^\dagger d_{i\alpha\downarrow} d_{i\alpha\uparrow} + h.c.) \end{aligned} \quad (3)$$

Here, we use  $c$  and  $d$  to identify the two  $S_4$  iso-spin components.  $\hat{n}_{\alpha i\sigma}^c = c_{\alpha i\sigma}^\dagger c_{\alpha i\sigma}$  and  $\hat{n}_{\alpha i\sigma}^d = d_{\alpha i\sigma}^\dagger d_{\alpha i\sigma}$ .  $\alpha$  labels the two sublattices of the iron square lattice with  $\alpha = 1, 2$ .  $U$  and  $U'$  are the direct intra- and inter-orbital Coulomb repulsions, respectively.  $J_H$  is the Hund term in  $H_{int}$  satisfying  $U' = U - 2J_H$ . The last term in  $H_{int}$  describes the spin-flip term of intro-orbital exchange and the pair hopping. Here we neglect the pair hopping term.

To obtain the possible ground-state in the undoped and underdoped cases, we apply a mean-field decoupling to the model in Eq.(3).  $H_{int}$  can be simply decoupled by defining the mean-field values of the diagonal operators,

$$\langle c_{\alpha\sigma}^\dagger c_{\alpha\sigma} \rangle = n_{\alpha\sigma}^c, \quad \langle d_{\alpha\sigma}^\dagger d_{\alpha\sigma} \rangle = n_{\alpha\sigma}^d \quad (4)$$

$$\langle c_{\alpha\uparrow}^\dagger c_{\alpha\downarrow} \rangle = \kappa_{\alpha}^c, \quad \langle d_{\alpha\uparrow}^\dagger d_{\alpha\downarrow} \rangle = \kappa_{\alpha}^d \quad (5)$$

If we assume that possible ordered states are only allowed to break translation symmetry up to four irons and let  $\alpha = 1, 2, 3, 4$  label sites in the four different sublattices respectively as shown in Fig.1(b), the mean-field Hamiltonian of Eq.(2) in the reciprocal space can be written as

$$\begin{aligned} H_{mf} = & H_0 + \sum_{k,\alpha,\sigma} [U n_{\alpha\sigma}^c + U' n_{\alpha\sigma}^d + (U' - J_H) n_{\alpha\sigma}^d] \hat{n}_{k\alpha\sigma}^c \\ & + \sum_{k,\alpha,\sigma} [U n_{\alpha\sigma}^d + U' n_{\alpha\sigma}^c + (U' - J_H) n_{\alpha\sigma}^c] \hat{n}_{k\alpha\sigma}^d \\ & - J_H \sum_{k,\alpha} \left[ \kappa_{\alpha}^c d_{k\alpha\downarrow}^\dagger d_{k\alpha\uparrow} + (\kappa_{\alpha}^d)^* c_{k\alpha\uparrow}^\dagger c_{k\alpha\downarrow} + h.c. \right] + C \end{aligned} \quad (6)$$

where  $C$  represents non-operator terms.

The above mean-field Hamiltonian can be numerically solved with a standard self-consistent procedure by minimizing free energy. During the iterative procedure of the self-consistent calculation, we enforced the average electron number per site at each step remains a constant, namely, keeps the density constant. We define the magnetization  $m_\alpha$  and polarization  $\Delta n_\alpha$  as

$$m_\alpha = (n_{\alpha\uparrow}^c - n_{\alpha\downarrow}^c) + (n_{\alpha\uparrow}^d - n_{\alpha\downarrow}^d) \quad (7)$$

$$\Delta n_\alpha = (n_{\alpha\uparrow}^c + n_{\alpha\downarrow}^c) - (n_{\alpha\uparrow}^d + n_{\alpha\downarrow}^d) \quad (8)$$

All different kinds of standard magnetic orders (such as C-AFM order, ferromagnetic order and antiferromagnetic order) and orbital orders (such as ferro-orbital order, staggered-orbital order and stripe orbital order) are included by above meanfield ansatz.

The zero-temperature phase diagram for the undoped case was obtained and shown in Fig. 3 (a). The C-AFM order was found to be stable in a broad and realistic range of interaction strength. Furthermore, the C-AFM orders exhibit differently depending on  $U$  and  $J_H/U$ . When  $J_H/U$  is large in a moderate value of  $U$ , no orbital-order was found. When  $J_H/U$  is small enough, a small staggered-orbital order coexists with the magnetic order. When  $U$  is large enough, as expected, the metallic C-AFM order becomes insulating. It is important to note that for a coexisting state with both C-AFM order and staggered orbital order, the corresponding magnetizations  $m_\alpha$  at the sites labeled in Fig.1(b) are  $m_{1/4} = m$  and  $m_{2/3} = -m$  and the orbital orders are given by  $\Delta n_i = m_o$  ( $i = 1, 2, 3, 4$ ). In Fig. 3 (b) (c) and (d), we plotted  $m$  and  $m_o$  as functions of  $U$ ,  $J_H/U$  and temperature  $T$ . From Fig. 3 (b), for the two undoped and 4.5% electron doped cases studied here,  $m$  jumps into a

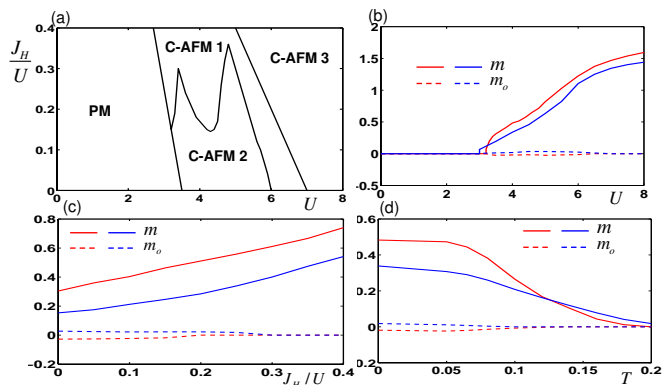


FIG. 3: (color online) (a) The zero-temperature mean-field phase diagram of the  $S_4$  effective model in the  $J_H/U$  vs  $U$  plane in undoped case. We denote ‘PM’ for the paramagnetic phase, ‘C-AFM 1’ for the metallic C-AFM phase, ‘C-AFM 2’ for the metallic C-AFM phase with a staggered orbital order and ‘C-AFM 3’ for the insulating C-AFM phase. (b), (c) and (d) show the C-AFM magnetization  $m$  and staggered orbital polarization  $m_o$  as the function of  $U$ ,  $J_H/U$  and  $T$ . The red color denotes the undoped case while the blue color denotes the 4.5% electron-doped case. The parameters are  $J_H/U = 0.15$  for undoped case and 0.25 for 4.5% electron doped case in (b),  $U = 4$  for both cases in (c), and  $J_H/U$  with the same values as (b) and  $U = 4$  in (d). The hopping parameters are indicated in the caption of Fig. 1.

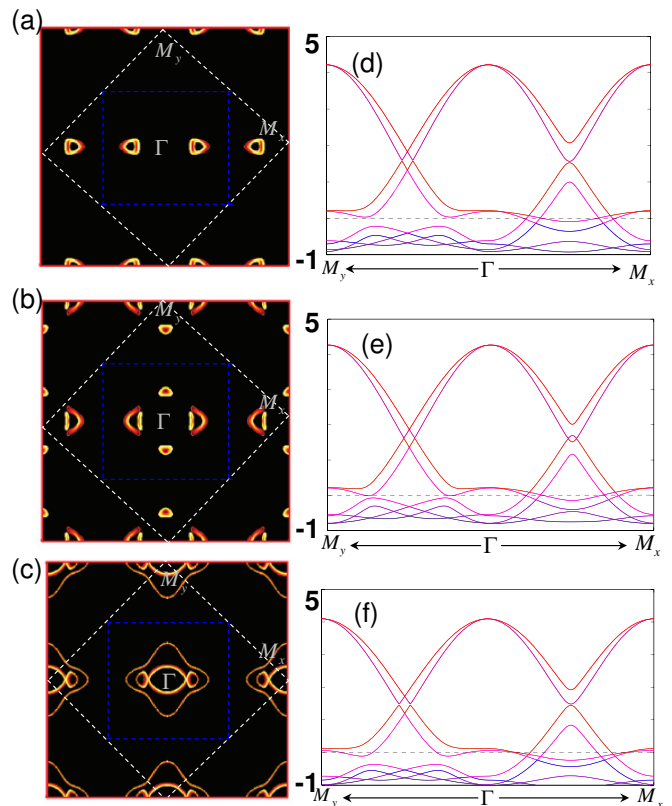


FIG. 4: (color online) The Fermi surfaces in C-AFM states are shown for some different interaction strength and doping. (a) the undoped case with  $U = 4$  and  $J_H/U = 0.15$ . (b) the undoped case with  $U = 3.5$  and  $J_H/U = 0.15$ . (c) the 4.5% electron-doped case with  $U = 4$  and  $J_H/U = 0.25$ . (d) (e) and (f) are the energy bands along  $\Gamma - M_x$  and  $\Gamma - M_y$  directions, respectively.

finite value at  $U \sim 3.2$  and  $\sim 3$  respectively, which means the transition from the PM to the C-AFM is a first order phase transition. From Fig. 3(c), the large  $J_H/U$  enhances the C-AFM order  $m$  and suppresses the staggered orbital order  $m_o$  in both undoped and underdoped cases. From Fig. 3 (d), increasing temperature suppresses both C-AFM order  $m$  and the staggered orbital order  $m_o$ , and so does the doping. We also find that increasing doping can continually reduce the C-AFM order  $m$  at low temperature. All the results are qualitatively consistent with the experimental observations[25].

The result that a staggered orbital order is favored over a ferro-orbital order stems from the  $S_4$  symmetry. As shown in Fig.1(a), each  $S_4$  iso-spin component is formed by two different types of orbitals in the two different sublattices of the iron square lattice. A staggered orbital order corresponds to the  $S_4$  symmetry breaking. Many theoretical proposals based on models with one-iron per unit cell emphasize the ferro-orbital order[26–28]. Therefore, in principle, the result can be used as a test for the  $S_4$  symmetry. Unfortunately, the staggered orbital order is rather small in our meanfield results.

*The formation of hot spots or small pockets in the C-AFM state:* To obtain further insights into the characters of the C-AFM ordered states, we investigated the Fermi surface construction which can be directly observed by APRES experiments. The reconstructed Fermi

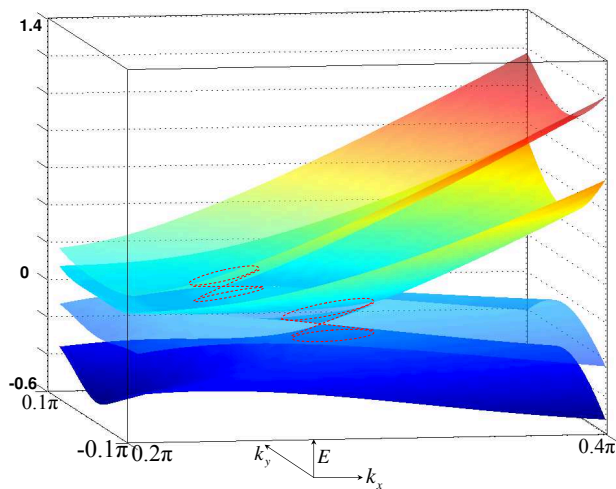


FIG. 5: (color online) The band structure around  $(\frac{\pi}{4}, 0)$  corresponding to Fig 4. (a) (d). The Dirac cone structures are marked with the red-dashed lines.

surfaces and bands of our model with different interaction strengths and doping cases are shown in Fig. 4. The interaction strength is chosen in the moderate strength range since iron-pnictides are most likely in intermediate coupling region. The Fermi surfaces in Fig. 4 (a), (b) and (c) show a close match to ARPES results measured in  $\text{BaFe}_2\text{As}_2$ [16],  $\text{NaFeAs}$ [17, 18] and  $\text{Ba}(\text{Fe}_{1-x}\text{Co}_x)_2\text{As}_2$ [15], respectively. Furthermore, the magnetization value in Fig. 4 (a) with  $m = 0.48$  for  $\text{BaFe}_2\text{As}_2$  is larger than the one in Fig. 4 (b) with  $m = 0.33$  for  $\text{NaFeAs}$ , which is also quantitatively consistent with experiments[25].

The remarkable character of reconstructed Fermi surfaces in  $\text{BaFe}_2\text{As}_2$  is the Dirac cone structures around the  $(\frac{\pi}{4}, 0)$  and  $(\frac{3\pi}{4}, 0)$ . Especially, the energy spectrum around the Dirac cone structures in Fig. 4 (d) are similar to the experimental fitting results[16]. From Fig. 4 (d), we can find that the Dirac cone structure around  $(\frac{\pi}{4}, 0)$  point is formed by a hole-like band from one  $S_4$  iso-spin component and a folded electron-like band from the other  $S_4$  iso-spin component while the Dirac cone structure around  $(\frac{3\pi}{4}, 0)$  point is formed by exchanging the contributions between two  $S_4$  iso-spin components.

In Fig. 5, we plotted the spectra around the  $(\frac{\pi}{4}, 0)$  point, where the Dirac cone structures are resolved with the red-dashed line. The Dirac cone structures were proposed as the universal character and robust with interaction strength and doping[23, 29]. Our results clearly show that the feature highly depends on quantitative parameter settings in a model and in general should be material-dependent.

*Discussion and conclusion:* Several LDA calculations have also noticed that some properties have to be understood in the base of the 2 Fe unit cell[30, 31]. From above results, we clearly see this importance reflected in the starting point of kinematics in analytic approaches. In most previous studies, in particular, analytic studies, calculations are performed in models with one iron per unit cell. In principle, the  $S_4$  symmetry kinematics is hidden in these models and can be revealed by performing a unitary transformation. However, when interactions are concerned and exact solutions are impossible, the search of meanfield order parameters highly depend on the base set in kinematics, which is the key reason why an explicit  $S_4$  construction becomes crucial. The result also suggests that many physical quantities in a symmetry broken state require new investigation.

It is also important to note that our calculation is performed in a tetragonal lattice. It is known that a lattice distortion or a tetragonal to orthorhombic lattice transition exists at a temperature higher than or equal to the magnetic transition temperature[25]. In general, the  $S_4$  symmetry is broken in the orthorhombic lattice. Our calculation does not include this aspect since the model is purely electronic and does not include an electron-lattice coupling. The lattice distortion is likely driven by pure electronic nematicism[9, 32–34] so that the qualitative results here will remain unchanged. Nevertheless, a full consideration of this aspect is needed in future.

In summary, we show that the  $S_4$  microscopic effective model characterized by a doubling of iron unit cell explains the puzzled band reconstruction in the magnetic state of iron-pnictides. The results provide a strong support to the kinematics described by the  $S_4$  symmetry.

*Acknowledgement:* JP thanks H. Ding, D.L. Feng and T. Xiang for useful discussion. The work is supported by the Ministry of Science and Technology of China 973 program(2012CB821400) and NSFC-1190024.

- 
- [1] Y. Kamihara, T. Watanabe, M. Hirano, and H. Hosono, *J. Am. Chem. Soc.* **130**, 3296 (2008).
  - [2] X. H. Chen, T. Wu, G. Wu, R. H. Liu, H. Chen, and D. F. Fang, *Nature* **453**, 761 (2008).
  - [3] G. F. Chen, Z. Li, D. Wu, G. Li, W. Z. Hu, J. Dong, P. Zheng, J. L. Luo, and N. L. Wang, *Phys. Rev. Lett.* **100** (2008).
  - [4] C. de La Cruz, Q. Huang, J. W. Lynn, J. Li, I. W. Ratcliff, J. L. Zarestky, H. A. Mook, G. F. Chen, J. L. Luo, N. L. Wang, et al., *Nature* **453**, 899 (2008).
  - [5] J. Zhao, D. T. Adroja, D. X. Yao, R. Bewley, S. L. Li, X. F. Wang, G. Wu, X. H. Chen, J. P. Hu, and P. C. Dai, *Nature Physics* **5**, 555 (2009).
  - [6] P. Dai, J. Hu, and E. Dagotto, *Nature Physics* **In Press** (2012).
  - [7] J. Dong, H. J. Zhang, G. Xu, Z. Li, G. Li, W. Z. Hu, D. Wu, G. F. Chen, X. Dai, J. L. Luo, et al., *Europhysics Letters* **83**, 27006 (2008).
  - [8] Q. Si and E. Abrahams, *Phys. Rev. Lett.* **101**, 76401 (2008).
  - [9] C. Fang, H. Yao, W. F. Tsai, J. P. Hu, and S. A. Kivelson, *Phys. Rev. B* **77**, (2008).
  - [10] J. Hu, B. Xu, W. Liu, N.-N. Hao, and Y. Wang, *Phys. Rev. B* **85**, 144403 (2012).
  - [11] T. Ma, H. Lin, and J. Hu, *Arxiv:1102.1381* (2012).
  - [12] F. Ma, Z.-Y. Lu, and T. Xiang, *Phys. Rev. B* **78**, 224517 (2008).
  - [13] F. Wang, H. Zhai, Y. Ran, A. Vishwanath, and D.-H. Lee, *Phys. Rev. Lett.* **102**, 47005 (2009).
  - [14] K. Kuroki, S. Onari, R. Arita, H. Usui, Y. Tanaka, H. Kontani, and H. Aoki, *Phys. Rev. Lett.* **101**, 087004 (2008).

- [15] M. Yi, D. H. Lu, J. G. Analytis, J. H. Chu, S. K. Mo, R. H. He, M. Hashimoto, R. G. Moore, I. I. Mazin, D. J. Singh, et al., *Phys. Rev. B* **80**, 174510 (2009).
- [16] P. Richard, K. Nakayama, T. Sato, M. Neupane, Y.-M. Xu, J. H. Bowen, G. F. Chen, J. L. Luo, N. L. Wang, H. Ding, et al., *Phys. Rev. Lett.* **104**, 0909.0574 (2010).
- [17] M. Yi, D. H. Lu, J.-H. Chu, J. G. Analytis, A. P. Sorini, A. F. Kemper, S.-K. Mo, R. G. Moore, M. Hashimoto, W. S. Lee, et al., *PNAS* **108**, 6878 (2011).
- [18] Y. Zhang, C. He, Z. R. Ye, J. Jiang, F. Chen, M. Xu, Q. Q. Ge, B. P. Xie, J. Wei, M. Aeschlimann, et al., *Phys. Rev. B* **85** (2012).
- [19] W. Z. Hu, Q. M. Zhang, and N. L. Wang, *Physica C Superconductivity* **469**, 545 (2009).
- [20] W. Z. Hu, G. Li, P. Zheng, G. F. Chen, J. L. Luo, and N. L. Wang, *Phys. Rev. B* **80**, 100507(R) (2009).
- [21] Z. G. Chen, R. H. Yuan, T. Dong, and N. L. Wang, *Phys. Rev. B* **81**, 100502 (2010).
- [22] S. J. Moon, J. H. Shin, D. Parker, W. S. Choi, I. I. Mazin, Y. S. Lee, J. Y. Kim, N. H. Sung, B. K. Cho, S. H. Khim, et al., *Phys. Rev. B* **81**, 205114 (2010).
- [23] Y. Ran, F. Wang, H. Zhai, A. Vishwanath, and D.-H. Lee, *Phys. Rev. B* **79**, 014505 (2009).
- [24] J. Hu and N. Hao, *Phys. Rev. X* **2**, 021009 (2012).
- [25] D. C. Johnston, *Adv. in Phys.* **59**, 803 (2010).
- [26] T. Saito, S. Onari, and H. Kontani, *Phys. Rev. B* **82**, 144510 (2010).
- [27] W. Lv, F. Krger, and P. Phillips, *Phys. Rev. B* **82**, 045125 (2010).
- [28] F. Kruuger, S. Kumar, J. Zaanen, and J. van den Brink, *Phys. Rev. B* **79**, 054504 (2009).
- [29] T. Zhou, D. Zhang, and C. Ting, *Phys. Rev. B* **81**, 052506 (2010).
- [30] C. Lin, T. Berlijn, L. Wang, C. Lee, W. Yin, and W. Ku, *Phys. Rev. Lett.* **107**, 257001 (2011).
- [31] V. Brouet, M. F. Jensen, P. H. Lin, and e. al., *Arxiv:1205.4513* (2012).
- [32] C. Xu, M. Miller, and S. Sachdev, *Phys. Rev. B* **78**, 20501 (2008).
- [33] I. Eremin and A. V. Chubukov, *Phys. Rev. B* **81**, 24511 (2010).
- [34] R. M. Fernandes, L. H. Vanbebber, S. Bhattacharya, P. Chandra, V. Keppens, D. Mandrus, M. A. McGuire, B. C. Sales, A. S. Sefat, and J. Schmalian, *Phys. Rev. Lett.* **105**, 157003 (2010).